

Emergence of Anderson localization in plasmonic waveguides

F. Rütting,* P. A. Huidobro, and F. J. García-Vidal

Departamento de Física de la Materia Condensada, Universidad Autónoma de Madrid, Madrid 28049, Spain

*Corresponding author: felix.rutting@uam.es

Received August 4, 2011; revised September 15, 2011; accepted September 29, 2011;
posted September 30, 2011 (Doc. ID 152276); published November 10, 2011

The propagation of surface plasmon polaritons in dielectric loaded waveguides with randomly placed scatterers is studied using both numerical simulations and a simplified transfer matrix framework. Despite the importance of losses in this system, we find fingerprints of the localized behavior of one-dimensional disordered systems. Furthermore, losses amplify the impact of the necklace states on the transport properties for systems not much larger than the localization length. The system presented here also offers the possibility to use localization effects for engineering purposes by means of deliberately introduced disorder. © 2011 Optical Society of America

OCIS codes: 240.6680, 130.2790.

The interference of multiply scattered waves gives rise to several interesting effects in the wave propagation through disordered media such as Anderson localization [1] (breakdown of diffusive transport due to disorder) and the existence of nonlocalized necklace states in the localized regime [2]. These interference effects are observable for any kind of wave, like quantum mechanical wave functions, electromagnetic (EM) waves [3–8], or, as a particular EM wave, surface plasmon polaritons (SPPs) [9,10]. In one-dimensional (1D) systems, wave propagation through disordered media is well understood, and the transfer matrix (TM) approach offers a powerful and elaborated formalism to treat the transport problem [11].

In this Letter we study the propagation of SPPs in dielectric loaded waveguides (DLWs) [12,13] equipped with randomly placed scatterers. Because of the large SPP propagation length in these waveguides [14,15], they are promising candidates for studying effects that rely on multiply scattered waves. Indeed, we have found both the emergence of Anderson localization and the formation of necklace states.

The structure under study is sketched in Fig. 1(a). A dielectric waveguide with a cross section of $600\text{ nm} \times 500\text{ nm}$ is placed on top of a gold surface. Then, disorder is introduced by a collection of scatterers, and these are realized by changing the refractive index of the dielectric in 50 nm wide slices. The mean distance between the scatterers is fixed to $1\text{ }\mu\text{m}$, while the disorder is introduced by means of random displacements of the individual scatterers. The displacements are normally distributed with a standard deviation of 100 nm . Figure 1(c) shows a plane cut along the direction of propagation of the DLW with the realization of the scatterers highlighted by solid lines. Dashed lines show the positions of the scatterers if the system was periodic. In contrast to systems with truly random disorder, these systems allow the design of samples with special realizations of disorder and hence the engineering of samples with predefined properties.

First, we will show that the transport properties of our three-dimensional (3D) system can be characterized by a 1D model within the TM framework. Only this simplified approach enables us to deal with the large number of realizations of the disorder, which is required for reliable

results and would be impossible to handle within a 3D model. Within the TM approach, systems with several scatterers are considered as consisting of several slices, each containing one scatterer. Hence, the reflection (r) and transmission (t) coefficients of one slice are needed. Once these coefficients are known, the calculation of the TM of the whole system is straightforward [11].

We have performed 3D finite-element method (FEM) calculations (with COMSOL Multiphysics) of systems without and with only one scatterer in order to determine the coefficients required by the TM approach. The

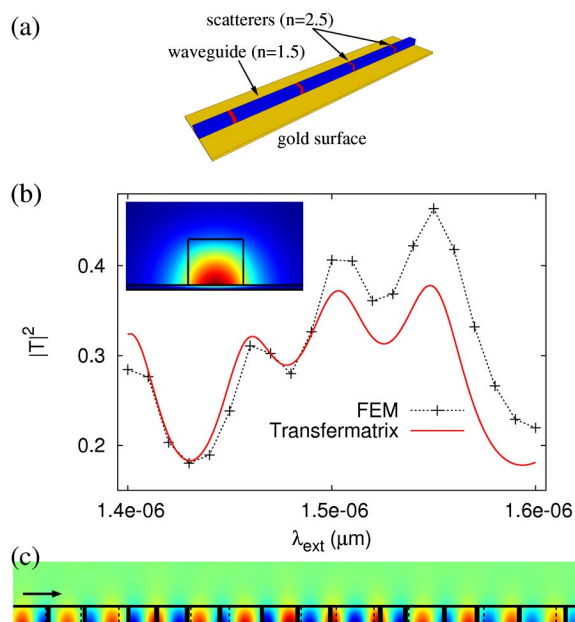


Fig. 1. (Color online) (a) Sketch of the system analyzed. A dielectric waveguide with refractive index of 1.5 (blue) is located on top of a gold surface. In the regions of the scatterers, the refractive index is changed to 2.5 (red). (b) Comparison between the transmission spectrum calculated with the TM approach and the results of the 3D FEM simulation for a system containing 15 scatterers. The inset shows the mode profile of a waveguide without any scatterers. (c) Field distribution (dominant magnetic component) at maximum transmission ($\lambda_{\text{ext}} = 1.55\text{ }\mu\text{m}$) (FEM simulation). Note that the scatterers are not located periodically (the dashed lines illustrate the locations of the periodic arrangement).

complex wave vectors of the system without scatterers allow us to calculate the phases of the coefficients and the absorption losses. On the other hand, the transmission and reflections probabilities and the scatterings losses are determined with the help of simulations of systems containing one scatterer. Our final results for the particular type of scatterer we are considering are

$$t = 0.963 \exp(-A_t + i\phi_t), \quad (1)$$

$$r_{\pm} = 0.2 \exp(-A_{r_{\pm}} + i\phi_{r_{\pm}}), \quad (2)$$

where the phases (ϕ) and absorption losses (A) depend on the wave vector and hence on the excitation wavelength λ_{ext} . Therefore, the reflection coefficients depend on λ_{ext} and, in addition, on the position of the scatterer inside the slice and on the propagation direction; + or -.

Having established the TM procedure, we have compared it with FEM simulations of a system of 15 scatterers for different excitation wavelengths. As shown in Fig. 1(b), the TM approach reproduces semiquantitatively the behavior of the transmission spectrum, even though there are of course some differences between the 3D calculations and the simplified 1D-one-mode model. However, this 1D TM formalism is accurate enough for discussing the SPP propagation in disordered DLWs.

The relevant length scale for describing localized systems is the localization length. This localization length characterizes the exponential decay of the transmitted energy, which is typical in the Anderson localization regime. In 1D systems any degree of disorder leads to localization. However, since losses are nonnegligible in the system studied here, the exponential decay of the intensity along the waveguide has several physical origins, and the decay has to be studied in more detail.

Within the TM approach the localization length l_{loc} is defined as [11]

$$l_{\text{loc}} = \lim_{L \rightarrow \infty} \frac{L}{\overline{\ln(R)}}, \quad (3)$$

with L being the sample length, and the mean of the logarithm of the resistance is defined as $\overline{\ln(R)} = -2\overline{\ln(|T|)}$. The absolute value of the transmission coefficient of the total system $|T|$ is the square root of the ratio of the transmitted intensity to the incident one. Figure 2(a) shows $L/\overline{\ln(R)}$ (averaged over 10^5 realizations) as a function of the sample size L , and for four cases: without losses, with only absorption losses, with only scattering losses, and with both losses. The limiting value in the lossless case determines the length scale of the disorder-induced localization $l_{\text{And}} = 35.6 \mu\text{m}$, while the losses lead to a reduced total decay length of $l_d = 12.4 \mu\text{m}$. This total decay length is well approximated by

$$l_d = [(l_{\text{And}})^{-1} + (l_{\text{abs}})^{-1} + (l_{\text{scat}})^{-1}]^{-1}, \quad (4)$$

where l_{abs} and l_{scat} are the decay lengths due to absorption and scattering losses, respectively. These loss-induced decay lengths can be extracted from the FEM simulations of just one slice, and for the system and

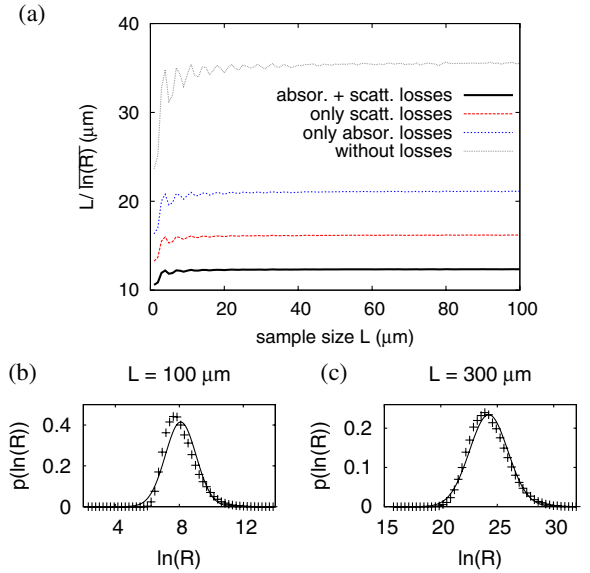


Fig. 2. (Color online) (a) $L/\overline{\ln(R)}$ as a function of the sample size L ; distribution of $\ln(R)$ for samples containing (b) 100 and (c) 300 scatterers. For comparison, normal distributions with the same mean values and standard deviations are also shown. All results are calculated for $\lambda_{\text{ext}} = 1.5 \mu\text{m}$.

wavelength used they are $l_{\text{scat}} = 30.2 \mu\text{m}$ and $l_{\text{abs}} = 52.7 \mu\text{m}$. Using these values and the Anderson localization length of $l_{\text{And}} = 35.6 \mu\text{m}$ in Eq. (4), we end up with $l_d = 12.5 \mu\text{m}$, which is in excellent agreement with the TM approach result including all losses ($l_d = 12.4 \mu\text{m}$).

For 1D, lossless, disordered systems much larger than the localization length, the logarithm of the resistance is normally distributed [11]. Hence, we have also investigated this distribution in our system. The results presented in Figs. 2(b) and 2(c) show that, for the sample sizes used, $\ln(R)$ is not perfectly normally distributed, but with an increasing sample size, the distribution equals more and more a normal distribution. The losses cause a lower limit for $\ln(R)$ and hence a deviation from the normal distribution, which becomes less important for larger systems. However, the fact that the distribution for an increasing sample size equals more and more a normal distribution indicates that the behavior of the disordered DLW lies within the Anderson localization regime. The results presented and discussed above illustrate that, even though losses are important in a plasmonic waveguide, clear fingerprints of the localized behavior of a 1D disordered system are present. Furthermore, the knowledge of the loss mechanism allows one to extract the Anderson localization length even from the results including losses.

Although 1D disordered systems are always in the localized regime, their transport properties are dominated by the existence of some extended states, the so-called necklace states, which show significantly enhanced transmittances compared to the localized states [6,11]. These states have a multiple resonance character and arise if two or more resonances appear at the same frequency. In Fig. 3(a) the transmission spectrum (calculated without losses) of a sample of 50 scatterers with a necklace state around $\lambda_{\text{ext}} = 1.484 \mu\text{m}$ is shown. Compared with the single resonances, the necklace state is

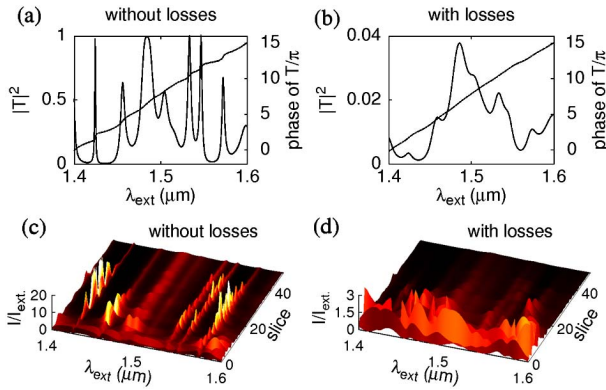


Fig. 3. (Color online) Transmission spectrum and wavelength-dependent intensity distribution of a disordered sample of 50 scatterers showing a necklace state around $\lambda_{\text{ext}} = 1.48 \mu\text{m}$ (a), (c) without losses and (b), (d) with losses.

wider, and also the increase of the phase of the transmission coefficient by 2π indicates that this resonance consists of two resonances. The qualitative differences between the resonances also emerge in the intensity distribution along the waveguide [see Fig. 3(c)]. A well-defined maximum appears for the single resonances, whereas the intensity along the DLW is more homogeneous in the necklace state.

In the previous paragraph, we discussed the necklace states without losses. Figures 3(b) and 3(d) show the transmission spectrum and the wavelength-dependent intensity distribution for the same sample as used before but now including losses. Because of the losses, all resonances are broadened, and the intensity along the waveguide is dominated by a loss-induced decay. Hence, the necklace-state criteria used before are no longer appropriate. However, the transmitted energy in the necklace state is much higher than the one in the single resonance. This is the typical behavior we found in many samples of the size used. While without losses, there are single and multiple resonances with a transmittance close to 1; by considering losses, the transmission coefficients of necklace states are significantly larger than those of single localized resonances. This can be explained by considering the intensity distributions at the different resonances without losses [see Fig. 3(c)]. The regions of largely enhanced intensity assigned to a long-lived single-resonance mode lead to high losses and hence to a reduced transmission. So even though the losses decrease the influence of multiply scattered waves, they increase the relative importance of necklace states with respect to single ones.

In conclusion, the transmission of SPPs in DLWs in which randomly placed scatterers are introduced shows

hallmarks of localization in 1D systems, even though losses are nonnegligible. Because of the more homogeneous intensity distribution along the waveguide in the necklace states, the losses enforce the impact of these states on the transmission compared to the single resonances. The emergence of Anderson localization in plasmonic waveguides with controllable disorder allows us to use localization effects to engineer specific samples with predefined properties. Thus, these systems can be used, for example, to enhance the light-matter interaction by using the regions of extremely enhanced fields, as has been demonstrated, for example, for disordered photonic crystals [8].

This work has been sponsored by the Spanish Ministry of Science under projects MAT2008-06609-C02 and DCSD2007-046-NanoLight. F. Rütting acknowledges support from the Deutsche Akademie der Naturforscher Leopoldina under grant LPDS 2009-52. P. A. Huidobro acknowledges financial support from the Spanish Ministry of Education through grant AP2008-00021.

References

1. P. W. Anderson, *Phys. Rev.* **109**, 1492 (1958).
2. J. B. Pendry, *J. Phys. C* **20**, 733 (1987).
3. P. W. Anderson, *Philos. Mag. B* **52**, 505 (1985).
4. D. S. Wiersma, P. Bartolini, A. Lagendijk, and R. Righini, *Nature* **390**, 671 (1997).
5. J. Bertolotti, S. Gottardo, D. S. Wiersma, M. Ghulinyan, and L. Pavesi, *Phys. Rev. Lett.* **94**, 113903 (2005).
6. J. Bertolotti, M. Galli, R. Sapienza, M. Ghulinyan, S. Gottardo, L. C. Andreani, L. Pavesi, and D. S. Wiersma, *Phys. Rev. E* **74**, 035602(R) (2006).
7. P. Sebbah, B. Hu, J. Klosner, and A. Z. Genack, *Phys. Rev. Lett.* **96**, 183902 (2006).
8. L. Sapienza, H. Thyrestrup, S. Stobbe, P. D. Garcia, S. Smolka, and P. Lodahl, *Science* **327**, 1352 (2010).
9. S. Grésillon, L. Aigouy, A. C. Boccara, J. C. Rivoal, X. Quelin, C. Desmarest, P. Gadenne, V. A. Shubin, A. K. Sarychev, and V. M. Shalaev, *Phys. Rev. Lett.* **82**, 4520 (1999).
10. F. Rütting, *Phys. Rev. B* **83**, 115447 (2011).
11. J. B. Pendry, *Adv. Phys.* **43**, 461 (1994).
12. B. Steinberger, A. Hohenau, H. Ditlbacher, A. L. Stepanov, A. Drezet, F. R. Aussenegg, A. Leitner, and J. R. Krenn, *Appl. Phys. Lett.* **88**, 094104 (2006).
13. T. Holmgaard, Z. Chen, S. I. Bozhevolnyi, L. Markey, A. Dereux, A. V. Krasavin, and A. V. Zayats, *Opt. Express* **16**, 13585 (2008).
14. T. Holmgaard and S. I. Bozhevolnyi, *Phys. Rev. B* **75**, 245405 (2007).
15. J. Grandidier, S. Massenet, G. C. des Francs, A. Bouhelier, J.-C. Weeber, L. Markey, A. Dereux, A. J. Renger, J. M. U. González, and R. Quidant *Phys. Rev. B* **78**, 245419 (2008).